Dynamics of Rigid and Flexible Constraints for Polymers. Effect of the Fixman Potential

Dennis Perchak,† J. Skolnick,‡ and Robert Yaris*

Department of Chemistry, Washington University, St. Louis, Missouri 63130.
Received July 10, 1984

ABSTRACT: Models of polymers can generally be divided into two classes: (a) flexible, wherein bond lengths and valence angles are constrained to nearly constant values by strong, harmonic potentials, and (b) rigid, wherein the constraints are geometric, i.e., fixed bond lengths and angles. In general, the statistical mechanics of such systems differ. By introduction of a compensating potential based on the metric determinant of the unconstrained coordinates (the Fixman potential), the rigid model can be made to reproduce the equilibrium flexible results. It is not clear whether the corresponding dynamics are also reproduced. The purpose of the present work is to investigate the effect of the Fixman potential on dynamics. We have performed Brownian dynamics simulations of three models of a *n*-butane-like molecule: flexible, rigid, and rigid-plus-Fixman potential. Results show that for certain autocorrelation functions of the dihedral angle, there is a definite, though small, difference in dynamics between the rigid and flexible models in the low-friction limit. At high friction the difference has decreased and the dynamics are essentially the same. The effect of the Fixman potential is minimal in both cases.

I. Introduction

Polymeric systems contain certain degrees of freedom (specifically bond lengths and valence angles) which under physically realistic conditions remain quite close to their equilibrium average values. Because of this, two distinct approaches to modeling the dynamic properties of polymers have arisen. One approach constrains the bond lengths and valence angles near their equilibrium values through the use of (reasonably realistic) harmonic potentials with very large force constants, termed here a flexible model. The large force constants associated with flexible models, however, yield very fast vibrational frequencies. For example, bond stretching frequencies can be on the order of 100 ps^{-1}. Since the time scale for numerical simulations is set by the fastest relaxational process, namely the bond stretching frequencies, flexible models require a very small integration time step. However, many aspects of the interesting physics (e.g., conformational transitions) occur on much longer time scales. The desire to concentrate computational power on the degrees of freedom of interest has led to a second approach in modeling of polymer dynamics in which bond lengths and valence angles are fixed exactly to some specified value. The use of such geometric constraints is termed a rigid model. Several versions of rigid polymer models have been developed. Examples include those of Fixman[1] and Pear and Weiner[2] and the various manifestations of the algorithm known as SHAKE.[3,4]

The classical equilibrium statistical mechanics of these two models, flexible and rigid, in general differ. Many authors have addressed this difference, in particular, Go and Scheraga[5,6] and Fixman.[1,7] In a rigid model the system is constrained to a hypersurface in phase space consistent with the fixed bond lengths and/or bond angles. The imposition of rigid constraints is manifested in the equilibrium statistical mechanical distribution function as a term based on the metric determinant of the hypersurface. This term is absent for the flexible model even in the limit where the force constants go to infinity. This difference between the flexible and rigid equilibrium distribution—even in the large force constant limit—though real, is somewhat counterintuitive. Part of the problem with intuition is that we usually assume that the large force constant limit of a flexible molecule is a rigid molecule, and we forget that one has an infinite amount of time to reach equilibrium. Thus, while a system with large force constants will stay close to the rigid constraint hypersurface in phase space for a while (perhaps even a "long" while), given enough time it will eventually sample the rest of phase space to yield the nonconstrained equilibrium distribution function. The intrinsic differences in equilibrium properties of rigid and flexible models have been explicitly demonstrated by computer simulations. Gottlieb and Bird[8] performed molecular dynamics simulations on a three-bead, two-bond molecule lacking any bond angle constraints whatsoever, and Pear and Weiner[2] performed Brownian dynamics simulations on a freely rotating, four-bead, three-bond molecule. In both cases when the rigid versions of these molecules were used, it was found that the distributions (of one bond relative to the other for the two-bond molecule and of the dihedral angle ϕ of the central bond for the three-bond molecule) were nonuniform. The flexible versions of both these molecules had uniform distributions. In particular, for the rigid version of the three-bond molecule of Pear and Weiner the distribution function of the dihedral angle ϕ was found to be proportional to the square root of the metric determinant, $g(\phi)$, in agreement with theory. It is important to note that although the magnitude of the differences between the distributions of the rigid and flexible models is small (maximum deviation from uniformity is 1.1 for the three-bead molecule and 1.3 for the four-bead one), the qualitative difference is great.

Fixman[1] had shown that the rigid model can be made to reproduce the equilibrium distribution of the flexible model by adding to the rigid model an additional effective potential (which will be explicitly given in section II for the case of *n*-butane) based on the metric determinant. Pear and Weiner[2] demonstrated that the inclusion of this potential (which they termed the Fixman potential) in the rigid-model simulations resulted in a uniform distribution for the dihedral angle ϕ.

In summary, the equilibrium (time-independent) statistical mechanics of rigid and flexible models of polymers differ and the physically correct flexible equilibrium results can be recovered by the addition of the Fixman potential to the rigid model. However, this says nothing at all about the correct way to treat the dynamic (time-dependent) properties of polymers. It is the purpose of the present work to investigate and compare through computer simulations the dynamics of these three models: flexible, rigid, and rigid-plus-Fixman potential. We will examine the

† Present address: Department of Macromolecular Science, Case Western Reserve University, Cleveland, OH 44106.
‡ Alfred P. Sloan Foundation Fellow.

0024-9297/85/2218-0519$01.50/0

differences in dynamic properties, if any, that exist between rigid and flexible models and, if there are differences, whether the inclusion of the Fixman potential enables us to recover the flexible results.

Helfand[9] has considered a simpler version of this question analytically by studying the motion of a system with only two degrees of freedom, one constrained and one unconstrained. He concluded that in the high-friction limit of the interaction of the system with its surroundings, use of the Fixman potential allows recovery of the results of the flexible dynamics but in the low-friction limit it may not. More recently, van Gunsteren and Karplus[10] have performed molecular dynamics on rigid and flexible versions of a protein model. They considered two kinds of rigid models, one in which the bond lengths are fixed by the bond angles are not and one in which both bond lengths and valence angles are fixed. Their results showed that if only the bond lengths were constrained, there were no significant differences with the flexible model. However, when both bond lengths and valence angles were rigidly constrained, they found large differences in the dynamics, particularly in a reduction of the dihedral angle conformational transition rates. Apparently this arose from steric effects due to repulsive van der Waals interactions between chain segments spatially close together but far apart along the chain contour, wherein the valence angle constraint effectively eliminated a path of steepest descent on the potential energy surface. It is important to realize that the differences in rigid and flexible models that we have discussed above do not come about by such an elimination of energetically favorable pathways. It is a purely statistical mechanical effect that arises because the momenta conjugate to the constrained coordinates are dependent on the dihedral angles. Thus, it is difficult to ascertain in the work of van Gunsteren and Karplus how much of the differences in dynamics are due to eliminating important pathways and how much are due to the statistical mechanical effects we have been discussing. Additionally, since their simulation of the protein was done with vacuum boundary conditions (no solvent interactions) and no use was made of the Fixman potential, one cannot directly compare with Helfand's analytic work which explicitly considers low- and high-friction limits.

It is our concern to investigate only the purely statistical mechanical questions and also, like Helfand, to consider a range of frictional effects. Our purpose here is to investigate the strictly pragmatic question whether in doing a computer simulation to study the dynamics of a polymer chain one can obtain meaningful results by using less than the fully flexible model. That is, can we get away with using a rigid model, must we correct this by using the Fixman potential, or do we really need the full dynamics of the flexible model? Thus we shall not artificially increase the difference between the rigid and the flexible model by increasing the masses of the end atoms.

The present work differs from a previous examination of the dynamics of flexible vs. rigid butane by Chandler[11] and co-workers in several respects. First of all, we solve the standard Langevin equation with a random force as opposed to stochastic equations equivalent to the Bohm–Gross kinetic equation. Secondly, we explicitly employ the Fixman potential in one of the models to examine its effect. Thirdly, in addition to the conformational transition kinetics of the dihedral angle we calculate the autocorrelation function of the dihedral angle with and without tumbling. One of the purposes in examining the correlation functions is to see whether there are qualitative differences in the dynamics; measurements such as transition rates will only reveal differences in magnitude of the time scales. Overall (see below), our qualitative conclusions are consistent with those of Chandler et al.

We have performed Brownian dynamics on a simple n-butane-line molecule with no repulsive interactions. The use of such a simple model with only one dihedral angle enabled us to examine the three versions of this molecule, flexible, rigid, and rigid-plus-Fixman potential, for several values of the solvent viscosity. The present work also differs from that of Pear and Weiner.[2] There, in an attempt to model the effect of the rest of a long chain on an interior three-bond section, they made the end atoms heavier than the interior ones by a factor of 10. This has the effect of overemphasizing the metric determinant if one is considering just a n-butane molecule. We treat all the beads as having the same mass. Additionally, they considered only the low-friction limit of the solvent viscosity and used a steric rotational potential having a single barrier, whereas we treat low and high friction and use a 3-fold symmetric rotational potential.

The outline of the remainder of this paper is as follows. In section II, we described each of the three models used and the method of simulation. In section III, we present the simulation results for transition rates and correlation functions. Section IV contains the conclusions.

II. Description of Dynamic Model

Flexible Model. Following Helfand et al.,[12a] we describe the n-butane-like molecule as a three-bond chain of four vertices or carbon centers labeled $i = 0, 1, 2, 3$. Bond lengths b_i ($i = 1, 2, 3$), where b_i is the distance between vertices i and $i - 1$, are kept near their equilibrium value b_0 by the harmonic potential

$$v_b(b_i) = \tfrac{1}{2}\gamma_b(b_i - b_0)^2 \tag{2.1}$$

γ_b is the bond stretching force constant. Similarly, valence angles θ_i ($i = 1, 2$), where θ_i is the angle given by the dot product of bond vectors $\mathbf{b}_i$ and $\mathbf{b}_{i+1}$, are kept near their equilibrium value θ_0 by the harmonic potential

$$v_\theta(\theta_i) = \tfrac{1}{2}\gamma_\theta(\cos\theta_i - \cos\theta_0)^2 \tag{2.2}$$

γ_θ is the angle bending force constant. For this model, there is only one dihedral angle ϕ describing bond rotation about the axis of the second bond. The torsional potential which hinders the rotation of the dihedral angle is given by the symmetric 3-fold potential

$$v_\phi(\phi) = \tfrac{1}{2}E_b(1 - \cos(3\phi)) \tag{2.3}$$

This potential does not accurately mimic a real n-butane molecule (steric hindrances prevent a rotation through 180°, and gauche and trans conformations should not be equal in energy) but it possesses enough of the qualitative features of n-butane to be sufficient for comparing the dynamics of rigid and flexible models. The parameters used in the simulations are listed in Table I. As regards the bond stretching and angle bending force constants, we have decreased their values by factors of 7 and 3, respectively, from more realistic estimates of these parameters. Since these force constants directly control the size of the time step used in the numerical integration of the equations of motion, lessening them allows for a larger time step and hence decreases the required computer time. As stated in the Introduction, the differences in the equilibrium statistical mechanics between rigid and flexible systems occur independently of the strength of the harmonic potentials. Moreover, as has also been demonstrated by Helfand et al.,[12b] decreasing the strength of the potentials by less than 1 order of magnitude should not qualitatively affect the dynamics, although it does affect the absolute

Table I
Parameters of the Simulations

property	flexible	rigid	units
m^a	0.014	0.014	kg/mol
$b_0{}^a$	0.153	0.153	nm
γ_b/m^a	2.512×10^9	na[d]	ns^{-2}
γ_θ/m^a	1.301×10^7	na[d]	J/kg
E_b/k_BT	3	3	
θ_0	90	90	deg
T	300	300	K
$\beta = \xi/m^b$			
1	1.93×10^3	1.95×10^3	ns^{-1}
2	2.32×10^4	2.34×10^4	ns^{-1}
3	4.63×10^4	4.68×10^4	ns^{-1}
$\delta t^{b,c}$			
1	0.00217	0.00640	ps
2	0.00217	0.00154	ps
3	0.00217	0.00051	ps

[a] Taken from ref 12a. [b] 1–3 refer to simulations 1–3, respectively; see text. [c] There were three values of the damping parameter used for which the values of the time step δt are also displayed. [d] na means not applicable.

magnitude of the transition rates, for example (as long as the bond angle bonding and bond stretching potentials are still strong). Another point to note from Table I is that, again for simplicity's sake, we have employed 90° valence angles instead of the usual tetrahedral ones. Also, $E_b/k_BT = 3$ (k_BT is Boltzmann's constant times the temperature) is somewhat low as a potential barrier; 4 or $5k_BT$ is a more reasonable value but the lower value allows for better statistics in the simulations.

Rigid Model. A complete description of this model is presented in ref 2; we only give a general picture here. The four carbon centers are again labeled $i = 0$–3 and the bond vectors, valence angles, and the single dihedral angle are denoted as before. However, instead of keeping b_i and θ_i nearly constant, they are fixed exactly to the values b_0 and θ_0, respectively. This is accomplished by constructing the equivalent mechanical system shown in Figure 1. There the n-butane molecule is composed of two linked, rigid bodies with vertices $i = 0, 1$ belonging to the first rigid body and $i = 2, 3$ to the second. The connecting rods on each of the rigid bodies are massless and of length b_0. The linkage between the two bodies consists of two rods of length $b_0/2$ (fixed to their respective bodies at an angle θ_0) and joined via a pin and socket mechanism that permits rotation about this bond. Utilizing the mathematical formalism in Wittenburg,[13] Pear and Weiner have developed the equations of motion for such a system which are in generalized rather than Cartesian coordinates.

The above model thus satisfies the bond length and angle constraints exactly. The steric interactions are introduced through the same potential $v_\phi(\phi)$ (eq 2.3) as is used in the flexible case. In this case the interaction appears as a torque internal to the pin and socket mechanism. The rigid model is thus comprised of the two linked rigid bodies which allow rotation around the bond b_2 governed by torques generated by the rotational potential v_ϕ.

Rigid-plus-Fixman Potential. As described in the Introduction, Fixman[1] has pointed out that recovery of the flexible equilibrium statistical mechanics can be obtained by introducing an additional rotational potential

$$v_{FP}(\phi) = k_BT \ln (g(\phi))^{1/2} \qquad (2.4)$$

$g(\phi)$ is the metric determinant for the phase space hypersurface resulting from constraints on the bond lengths and valence angles. For the three-bond chain with 90° valence angles this determinant is[2]

$$g(\phi) = C(35 + 4 \cos \phi - 16 \cos^2 \phi + \cos^4 \phi) \qquad (2.5)$$

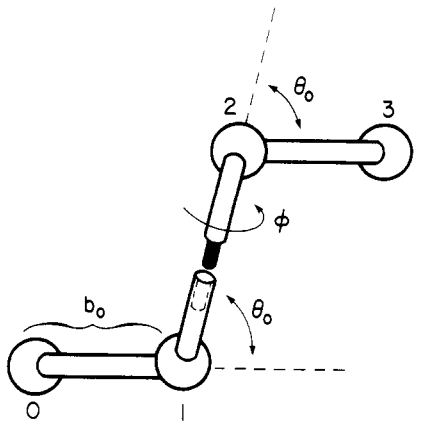

Figure 1. Rigid model of Pear and Weiner consisting of fixed bond lengths and valence angles and a pin and socket mechanism (dotted outline) to allow for dihedral angle variation.

where C is a constant. The rigid-plus-Fixman-potential model is formed by adding to the rigid model an additional torque given by $\partial v_{FP}(\phi)/\partial\phi$.

Brownian Dynamics. In all three versions of the model, we assume that the n-butane is in dilute solution in a solvent and account for the interaction of the solvent with the n-butane via the Langevin equation. This equation adds to the regular equations of motion a systematic damping term specified by a friction coefficient ξ and a random fluctuating force $\mathbf{A}_i(t)$ acting on each carbon center. The random force is Gaussianly distributed with zero mean and covariance

$$\langle \mathbf{A}_i(t)\mathbf{A}_j(t') \rangle = 2\xi k_BT\mathbf{I}\delta_{ij}\delta(t - t') \qquad (2.6)$$

where $\mathbf{I}$ is the 3×3 identity matrix.

For the flexible model we have employed the numerical procedures due to Helfand[14] and Greenside and Helfand[15] which are an extension of the Runge–Kutta method to stochastic differential equations such as the Langevin equation; in particular the method used here is to second order. For the rigid model we have used the method employed by Pear and Weiner[2] and use a fourth-order Runge–Kutta method to extend a solution of the Langevin equation from time t to time $t + \delta t$ without the Langevin force. Velocities were then incremented with a random impulse with the statistical characteristics of eq 2.6. Values of the friction coefficients and time steps used for the simulations are summarized in Table I.

III. Simulation Results

For each of three models we ran the simulations for three values of the friction coefficient $\beta = \xi/m$ given in Table I and shall refer to the three simulations by 1–3, respectively. If we consider the harmonic part of the curvature of v_ϕ, we can define a critical damping $\beta_c = 2.03 \times 10^4$ ns^{-1}. Thus, we have one set of runs, run 1, that is underdamped (by a factor of about 10), one set just above critical damping, run 2, and one set that is overdamped (by a factor of 2.3), run 3. We should point out that a more realistic value of β would be $5\beta_c$.

Initially, in order to check equilibration, we looked at the equilibrium population distribution with respect to the torsional angle for each of the cases. Simulations were run sufficiently long so that dynamical averages had stabilized. Because of the smallness of the Fixman potential (see below, especially Figure 7), the differences in the equilibrium distributions were small, being on the order of the noise level.

We begin with a presentation of calculated transition rates of the dihedral angle ϕ for the three models: flexible,

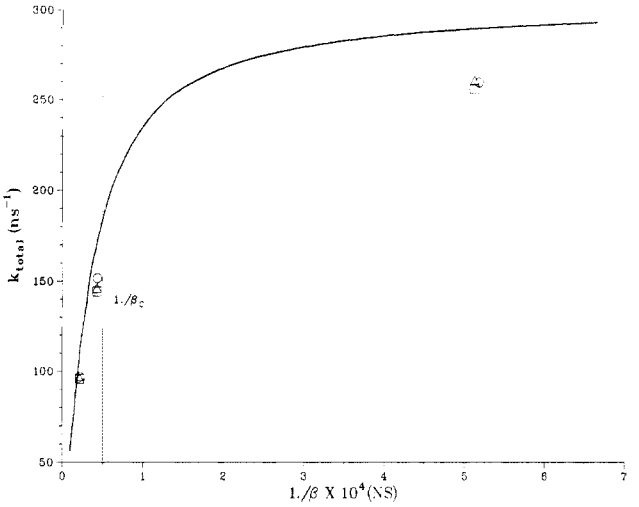

Figure 2. Total transition rate k vs. the damping coefficient β^{-1}. Circles represent the flexible model, squares the rigid model, and triangles the rigid-plus-Fixman-potential model. The solid line is from Skolnick and Helfand's extension of Kramer's rate theory (ref 16). The vertical dotted line represents critical damping, $\beta_c = 2.03 \times 10^4$ ns^{-1}.

rigid, and rigid-plus-Fixman potential. Rates were calculated by counting only those transitions that crossed the entire barrier region between minima, i.e., those where ϕ went from $\phi^* - \pi/6$ to $\pi^* + \pi/6$ or vice versa (ϕ^* is the position of a maximum of v_ϕ). Since, for our choice of the torsional potential, all three minima are equivalent, we calculated the total transition rate which includes trans to gauche, gauche to trans, etc. In Figure 2 the circles represent results of the flexible simulations while the squares are for the rigid and the triangles rigid-plus-Fixman-potential simulations, respectively. The solid line is from a calculation of the transition rates using a multidimensional extension of Kramer's rate theory due to Skolnick and Helfand[16] for a flexible-polymer model. We first note that for all three sets of runs there are essentially no differences in transition rates among the simulations. Next, we see that the transition rates of the simulations are approximately 10–16% lower than the corresponding theoretical values and thus are in good agreement with Kramer's rate theory. If we taken the square root of the inverse of the total number of transitions counted by the simulations as a rough estimate of the error in measuring the rates, then our error ranges from 5% (underdamped) to 10% (overdamped). Thus, even though Figure 2 shows a difference between simulation and theoretical rates that is roughly independent of the damping coefficient, it is difficult to conclude that the independence is real and would continue if one went to higher values of β. However, it is clear that the rates for all the simulations are equivalent and that the difference with theory is relatively small.

We next calculated some typical types of autocorrelation functions. In particular, consider a unit vector $\hat{b}(t)$ directed along bond b_3 at time t. The correlation functions that we measured were

$$P_1(t) = \langle \hat{b}(t)\cdot\hat{b}(0) \rangle \tag{3.1}$$

$$P_2(t) = \langle \tfrac{1}{2}\{3[\hat{b}(t)\cdot\hat{b}(0)]^2 - 1\} \rangle \tag{3.2}$$

i.e., the first and second Legendre polynomials of the change in direction of bond b_3; brackets represent time averages. P_1 and P_2 are given in terms of vectors associated with the orientation of bonds in n-butane so we must specify a reference frame in order to do the calculations. We evaluated P_1 and P_2 for a space-fixed reference frame within both overall molecular tumbling and rotation about the bond b_2 contribute to the correlation functions. We also used a molecular-fixed system (specifically, a reference frame attached to the bond b_1) wherein only rotation about b_2 contributes.

Figure 3 shows $P_1(t)$ evaluated in the space-fixed reference system for the three simulation models (flexible, rigid, and rigid-plus-Fixman potential) for both the underdamped ($\beta/\beta_c = 0.095$, run 1) and overdamped ($\beta/\beta_c = 2.3$, run 3) cases. Figure 4 deicts $P_2(t)$ for the same conditions. In both these figures, a solid line represents the flexible model, a dashed line the rigid model, and a dotted line the rigid-plus-Fixman-potential model. For the

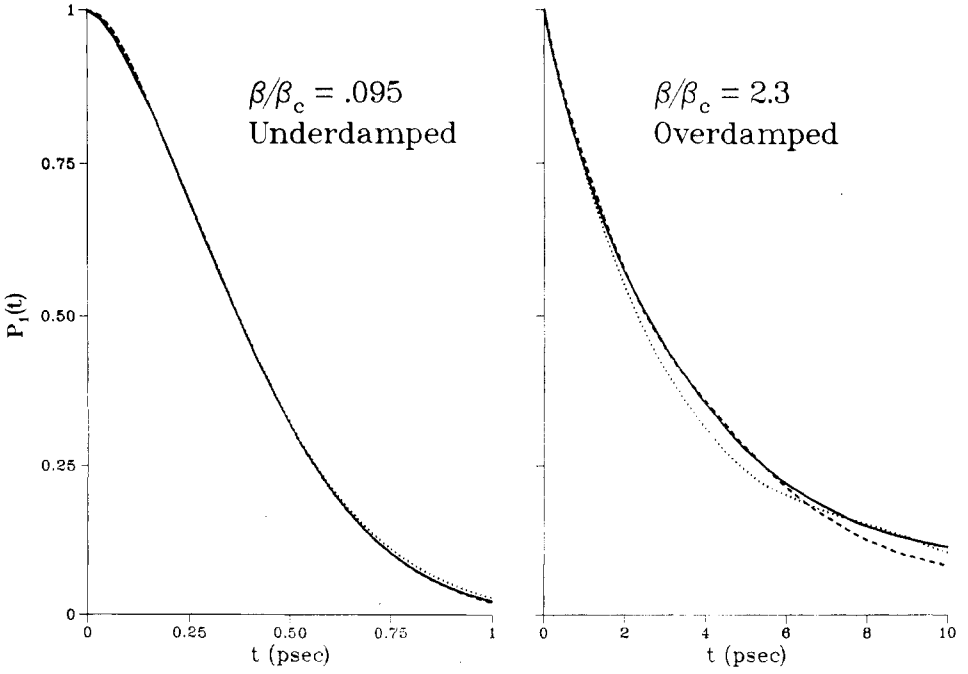

Figure 3. $P_1(t)$ vs. t evaluated in the space-fixed reference frame. The solid lines represent the flexible-model results, the dashed lines are for the rigid model, and the dotted lines are for the rigid-plus-Fixman-potential model. The plot on the left is for an underdamped friction coefficient and on the right for an overdamped one.

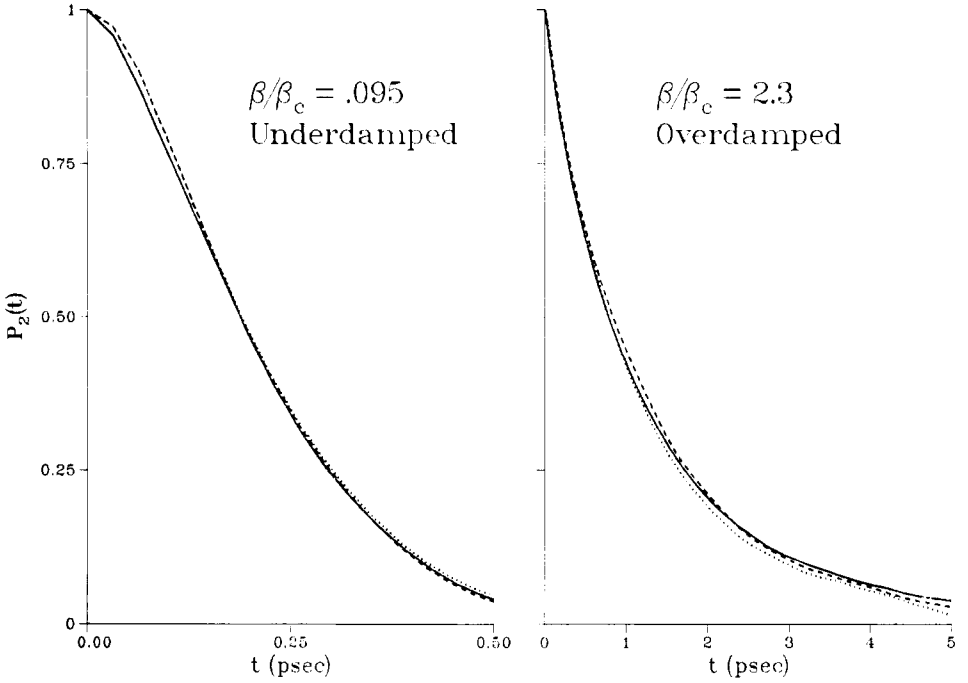

Figure 4. $P_2(t)$ vs. t for the same conditions as in Figure 3. The solid lines represent the flexible-model results, the dashed lines are for the rigid model, and the dotted lines are for the rigid-plus-Fixman-potential model.

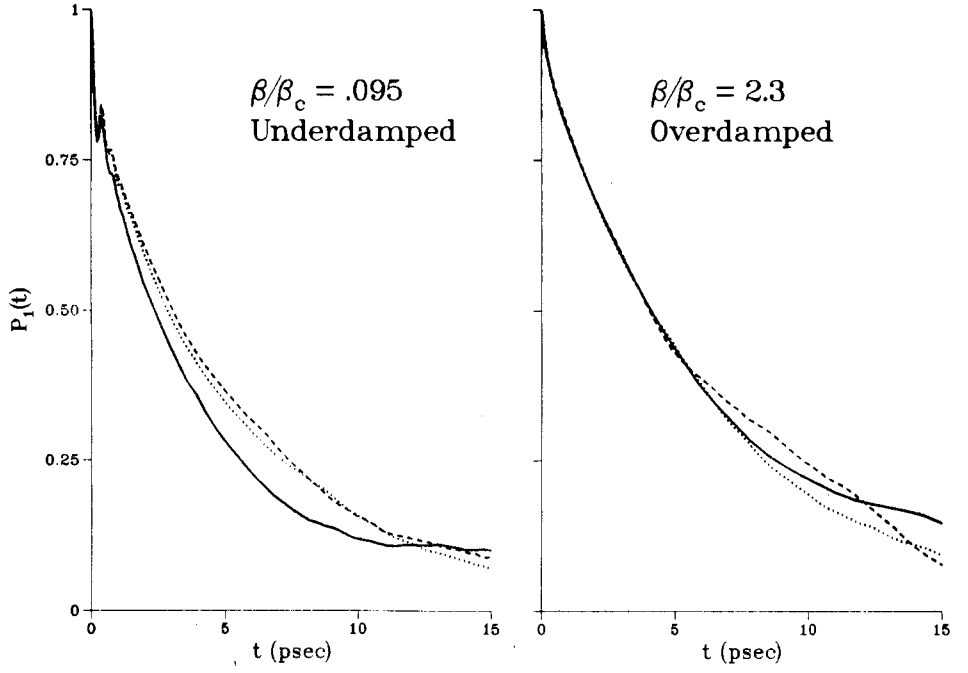

Figure 5. $P_1(t)$ vs. t evaluated in the molecule-fixed reference frame. The solid lines represent the flexible-model results, the dashed lines are for the rigid model, and the dotted lines are for the rigid-plus-Fixman-potential model.

underdamped cases on P_1 and P_2, all three simulations have identical relaxation curves. Similarly, the overdamped cases on P_1 and P_2 also show essentially the same relaxation. For the overdamped cases, there appears to be a slight tendency for the rigid-plus-Fixman-potential model to relax faster than the rigid model (as well as the flexible one). This is in accord with the work of Helfand on a simple two degrees of freedom model where he calculated that for high friction the rigid-plus-Fixman potential model behaves like the flexible model, while in the low friction limit these may be differences between the two models (but what kind is not easily determined). However, all three curves are in reality quite close so that one would most likely consider all three curves to be identical within the error of the simulations. We also note that the relaxation times for all three models increase greatly for the overdamped cases as compared to the underdamped ones, which is a physically reasonable result.

We next turn to the molecule-fixed reference frame for evaluating the correlation functions. Figures 5 and 6 depict these results for P_1 and P_2, respectively, again, for all three models with under- and overdamped friction coefficients. Here we see that for the underdamped situation (both P_1 and P_2), there is a definite difference between the rigid and flexible simulations, while there is almost no difference between the two rigid models. The differences between the rigid and flexible simulations, however, are not drastic in nature. For the overdamped situation, the two rigid models seem to be collapsing onto the flexible curve. The rigid-plus-Fixman-potential model tends to relax faster

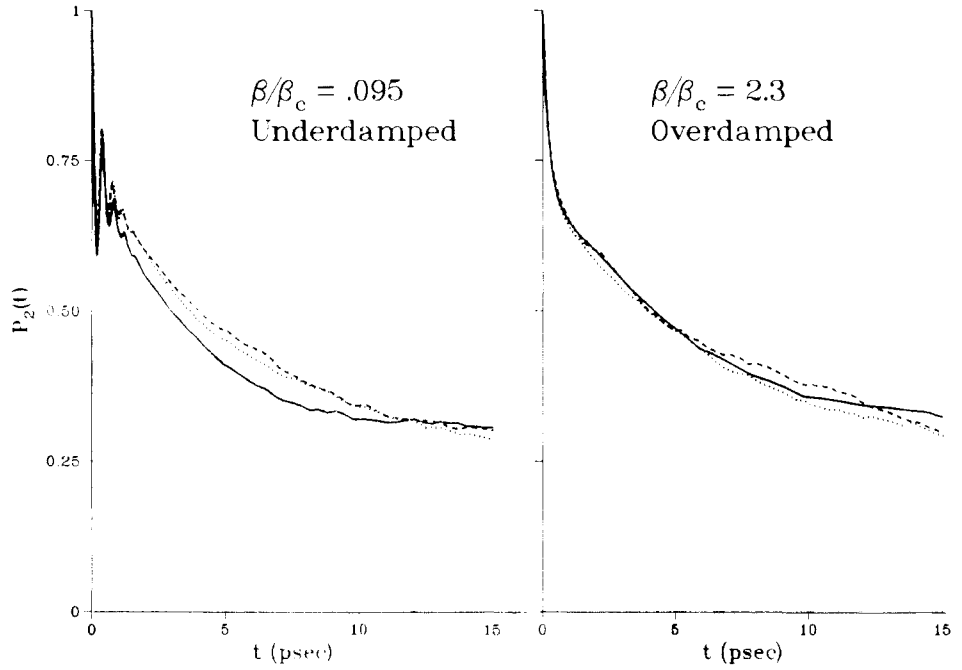

Figure 6. $P_2(t)$ vs. t for the same conditions in Figure 5. The solid lines represent the flexible-model results, the dashed lines are for the rigid model, and the dotted lines are for the rigid-plus-Fixman-potential model (note: the infinite time limit of P_2 is 0.25).

than the rigid model as was previously the case, but again, all three curves are very close and any differences are most likely within the noise level of the simulations.

There are several other points to be noted. For the underdamped case, the correlation functions show oscillations at short times (one oscillation for P_1; two or three for P_2). These oscillations represent collisions with the barrier of the torsional rotational potential and the time scale ($\sim$0.3 ps) of the collisions agrees with that for an oscillator in a well whose curvature is given by the harmonic part of v_ϕ. These oscillations are wiped out by the strong frictional effects in the overdamped situation.

IV. Discussion

To investigate the differences between the dynamics of rigid and flexible constraints for polymers, we have performed Brownian dynamics simulations of several models of a *n*-butane-like molecule. The models were as follows: (a) flexible—bond lengths and valence angles kept nearly constant by strong, harmonic potentials; (b) rigid—bond lengths and angles kept constant by geometric constraints; (c) rigid-plus-Fixman potential—the rigid model plus an extra dihedral angle rotational potential based on the metric determinant of the unconstrained coordinates. We performed computer simulations on these three models for several values of the friction coefficient corresponding to low friction (underdamped) and high friction (overdamped). From the simulations, we calculated and compared conformational transition rates and autocorrelation functions for the three models. We briefly summarize the results.

A comparison of transition rates for the three models showed no differences. This was true for all three values of the damping constant used. The transition rates of all three models were in good agreement with the Skolnick–Helfand extension of Kramer's rate theory, showing rates approximately 10–16% lower than the theoretical values.

The first and second Lengendre polynomials (P_1 and P_2, respectively) of the change in direction of the bond vector $\hat{b}_3$ were calculated. These were evaluated in a space-fixed reference system (which includes the effects of molecular tumbling) and in a molecular-fixed frame (which excludes tumbling). We presented results for the underdamped and overdamped cases. For P_1 and P_2 evaluated in the space-fixed reference frame, there were no differences among the relaxation curves for all three models for either under- or overdamped values of the friction constant. When P_1 and P_2 are evaluated in the molecular-fixed frame, in the underdamped case the two rigid simulations were identical but they both relaxed more slowly than their flexible counterparts. This difference is not drastic but there is a clear separation of relaxation behavior between the rigid and flexible models. For overdamped β the relaxation characteristic of all three models is essentially the same. There is a slight tendency for the rigid-plus-Fixman-potential model to relax more quickly than the rigid model but all three curves are so close that it is difficult to make any definite statements about this trend.

The fact that the rigid and rigid-plus-Fixman-potential simulations differ so little is perhaps not surprising. Consider Figure 7, where we have plotted the dihedral potential divided by k_BT vs. ϕ due to the torsional potential (solid line), due to the Fixman potential (dashed line), and due to the two combined (dotted line). We see that the Fixman potential is a very small perturbation on the torsional potential, and thus we do not expect (and do not see) any major differences between the rigid and rigid-plus-Fixman-potential simulations. Helfand has analytically studied a simple system with only two degrees of freedom, one constrained and the other unconstrained.[9] His analysis concluded that at low friction, the Fixman potential may not be enough to recover the flexible dynamics while at high friction it should suffice. Our simulation results are basically consistent with this picture. At low friction, the Fixman potential makes almost no difference. At high friction, however, what appears to be happening is that all three simulations are collapsing to the same relaxation curve. The rigid-plus-Fixman-potential model does relax faster than the rigid alone, but since all the curves are so close (essentially within the noise level of the simulations), the best we can say is that the results are consistent with Helfand's conclusions.

We feel that there are two main conclusions to be drawn from the present work. The first is that, in the high-

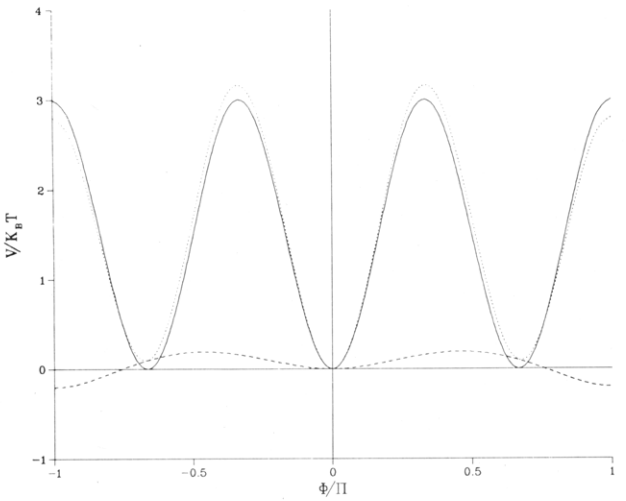

Figure 7. Potential about bond b_2 (in units of k_BT) vs. ϕ. The solid line represents the bare torsional potential v_ϕ defined in eq 2.3, the dashed line is the Fixman potential given by eq 2.4, and the dotted line is the torsional-plus-Fixman potential.

friction limit (overdamped), the dynamics of rigid and flexible models of *n*-butane do not differ significantly. Secondly, in the low-friction limit (underdamped) where the dynamics do differ (although only slightly), the addition of the Fixman potential is of no help. Since the overdamped case is the physically realistic situation, we conclude that the dynamics of rigid and flexible models of *n*-butane are essentially equivalent.

Unfortunately, one cannot automatically generalize from the case of *n*-butane to longer chains. The reason is that butane, because of its single dihedral angle, has only one long time scale associated with it (except for overall rotation and translation). Long chains, on the other hand, will have many different time scales because of the larger number of soft modes. It is not clear whether the rigid model will accurately reproduce the flexible model in these cases. Such a study is the subject of future work.

Acknowledgment. This work was supprted in part by a grant from the National Science Foundation Polymer Program (Grant DMR-8303197) and from the Biophysical Program (Grant PCM-8212404). Acknowledgment is also made to the donors of the Petroleum Research Fund, administered by the American Chemical Society, for partial support of the research. We thank Gene Helfand for his very helpful discussions and suggestions.

References and Notes

(1) Fixman, M. *J. Chem. Phys.* **1978**, *69*, 1527, 1538.
(2) Pear, M. R.; Weiner, J. H. *J. Chem. Phys.* **1979**, *71*, 212; **1980**, *72*, 3939.
(3) Ryckaert, J.-P.; Ciccotti, G.; Berendsen, H. J. C. *J. Comput. Phys.* **1977**, *23*, 327.
(4) van Gunsteren, W. F.; Berendsen, H. J. C. *Mol. Phys.* **1977**, *34*, 1311.
(5) Go, N.; Scheraga, H. A. *J. Chem. Phys.* **1969**, *51*, 4751.
(6) Go, N.; Scheraga, H. A. *Macromolecules* **1976**, *9*, 535.
(7) Fixman, M. *Proc. Natl. Acad. Sci. U.S.A.* **1974**, *71*, 3050.
(8) Gottlieb, M.; Bird, R. B. *J. Chem. Phys.* **1976**, *65*, 2467.
(9) Helfand, E. *J. Chem. Phys.* **1979**, *71*, 5000.
(10) van Gunsteren, W. F.; Karplus, M. *Macromolecules* **1982**, *15*, 1528.
(11) Montgomery, J. A.; Holmgren, S. H.; Chandler, D. *J. Chem. Phys.* **1980**, *73*, 3688.
(12) (a) Helfand, E.; Wasserman, Z. R.; Weber, T. A. *Macromolecules* **1980**, *13*, 526. (b) Helfand, E.; Wasserman, Z.; Weber, T.; Skolnick, J.; Runnels, J. H. *J. Chem. Phys.* **1981**, *75*, 4441.
(13) Wittenburg, J. "Dynamics of Systems of Rigid Bodies"; Teubner: Stuttgart, 1977.
(14) Helfand, E. *Bell Syst. Tech. J.* **1979**, *58*, 2289.
(15) Greenside, H. S.; Helfand, E. *Bell Syst. Tech. J.* **1981**, *60*, 1927.
(16) Skolnick, J.; Helfand, E. *J. Chem. Phys.* **1980**, *72*, 5489.

Measurement of the Correlation Hole in Homogeneous Block Copolymer Melts

Frank S. Bates†

AT&T Bell Laboratories, Murray Hill, New Jersey 07974. *Received August 10, 1984*

ABSTRACT: Homogeneous block copolymer melts are predicted to exhibit a decrease in interchain segment correlation (a "correlation hole") at wavevectors corresponding to a polymer coil radius. Small-angle neutron scattering data are presented which demonstrate this effect in two 1,4-polybutadiene–1,2-polybutadiene diblock copolymers. These results are quantitatively predicted by the mean-field theory of Leibler, thereby providing a new method for determining the Flory interaction parameter χ in binary polymer blends. χ was found to be dependent on sample composition, which can be attributed to equation-of-state contributions to the mixing free energy.

Introduction

A system of undiluted, amorphous homopolymers of sufficiently high index of polymerization ($N \gg 1$) is composed of ideal (Gaussian) chains, for which the mean squared radius of gyration, $R^2 = Na^2/6$, is defined in terms of an effective segment (Kuhn) length, a. In the case where every chain contains a block of labeled and a block of unlabeled segments, the probability of bringing like segments from separate chains into the same vicinity is reduced, since molten polymers are nearly incompressible. This depletion of interchain segment–segment correlation is called the correlation hole[1] and results in a peak in the measured correlation function, $S(Q)$, at a scattering wavevector of $QR \sim 1$. Small-angle neutron scattering (SANS) measurements of polystyrene samples containing blocks of deuterium-labeled segments have confirmed the prediction of the correlation hole for noninteracting chains.[2] Homogeneous block copolymers containing blocks of chemically different segments between which there exists a nonzero energy of interaction, typically defined in terms of the Flory parameter χ, have not been so examined. Leibler[3] has expanded on the concept of the correlation hole in noninteracting chains and calculated the correlation function for diblock copolymers in the

† Present address: Department of Chemical Engineering, California Institute of Technology, Pasadena, CA 91125.

0024-9297/85/2218-0525$01.50/0